

Article

High Compact, High Quality Single Longitudinal Mode Hundred Picoseconds Laser Based on Stimulated Brillouin Scattering Pulse Compression

Zhenxu Bai, Yulei Wang *, Zhiwei Lu *, Hang Yuan †, Zhenxing Zheng †, Sensen Li, Yi Chen, Zhaohong Liu, Can Cui, Hongli Wang and Rui Liu

Received: 1 December 2015; Accepted: 15 January 2016; Published: 20 January 2016

Academic Editor: Totaro Imasaka

National Key Laboratory of Science and Technology on Tunable Laser, Harbin Institute of Technology, Harbin 150001, China; baizhenxu@hotmail.com (Z.B.); yh6082110401@126.com (H.Y.); zxzhen2003@163.com (Z.Z.); 15004540383@163.com (S.L.); evanchan1986@gmail.com (Y.C.); lzh_hit@126.com (Z.L.); cuicanzz.hit@gmail.com (C.C.); wanghongli4713@163.com (H.W.); lrxiaokiss@126.com (R.L.)

* Correspondence: wyl@hit.edu.cn (Y.W.); zw_lu@sohu.com (Z.L.); Tel.: +86-0451-8641-2759 (Y.W. & Z.L.)

† These authors contributed equally to this work.

Abstract: A high beam quality hundred picoseconds single-longitudinal-mode (SLM) laser is demonstrated based on stimulated Brillouin scattering (SBS) pulse compression and aberration compensation. Flash-lamp-pumped Q-switched Nd³⁺:Y₃Al₅O₁₂ (Nd:YAG) SLM laser with Cr⁴⁺:Y₃Al₅O₁₂ (Cr⁴⁺:YAG) as a saturable absorber is used as the seed source. By combining master-oscillator-power-amplifier (MOPA), a compact single-cell with FC-770 as working medium is generated as pulse compressor. The 7.8 ns SLM laser is temporally compressed to about 450 ps, and 200 mJ energy is obtained at 1064 nm without optical damage. The energy stability is better than 3% with beam quality factor M^2 less than 1.8, which makes this laser system an attractive source for scientific and industrial applications.

Keywords: picosecond laser; stimulated Brillouin scattering (SBS); pulse compression; high energy

1. Introduction

Ultrashort lasers with high energy and high power intensity have wide application prospects, such as laser induced plasma (LIP), space debris detection, laser peening, nonlinear optics, spectroscopy, and laser processing [1–5]. Generally, the so-called ultrashort pulse refers to the lasers with pulse width between nanosecond (~ns) and femtosecond (~fs). In terms of output characteristics, the picosecond laser has shorter pulse width and high peak power compared with nanosecond laser; on the other hand, compared with the femtosecond laser, the picosecond laser also has higher stability and easily achieves high energy. These characteristics make picosecond lasers more attractive for many applications.

At present, mode-locking technique is the main method for obtaining picosecond pulses with pulse energies a few nano-joule and repetition rate up to hundreds MHz [6–8]. It is necessary to achieve significant higher pulse energies while keeping the pulse duration amplifiers. In this case, regenerative amplifiers are commonly used to strongly amplify selected individual optical pulses from a mode-locked train emitted by oscillators and allow multi-pass through the gain medium placed in an optical resonator. Although the amplification gain is about 10^5 or 10^6 of the injected energy, the maximum energy obtained after the regenerative amplifier is just in the order of few milli-joules as reported [9–12]. In addition, the structure of the regenerative amplifier is very complicated with poor stability. Such a low single pulse energy is still unable to meet the needs of a lot of applications.

Moreover, in some specific areas, ultra-short pulse lasers with single longitudinal mode (SLM) are often required such as optical sensing, laser radar and optical frequency standard. That means that the mode-locked picosecond laser cannot meet the application requirements in those fields.

The stimulated Brillouin scattering (SBS) phenomenon was discovered decades ago and has been widely used in phase stabilization, pulse compression, beam combination and ultrafast pulse shaping [13]. Among them, in the field of laser pulse compression, SBS is an effective method to compress a long pulse for its high energy reflectivity and high compression ratio. In particular, SLM output can be obtained by SBS pulse compression due to the Stokes spectrum is the result of convolution of the pump spectrum and the SBS medium gain spectrum. The temporal schematic diagram of SBS pulse compression process is shown in Figure 1. The medium of SBS cell can be liquid, gas or solid. By SBS pulse compression, Stokes light with pulse width of few and sub-nanoseconds can be obtained [14–16]. In order to achieve pulse compression, different types of SBS compressor were designed including taped waveguide, one-cell geometry, oscillator amplifier, compact two cell, scalable two cell, and so on. Three kinds of the most widely used structures are schematically depicted in Figure 2. Figure 2a shows the original single-cell pulse compressor with long focal-length lens. This structure suffers disadvantages of easily occurring optical breakdown and low compression ratio that make it unsuitable for practical application [17,18]. Figure 2b is the basic two-cell structure with two separate cells: one relatively short cell as a generator, and the other as an amplifier. A short focal lens is adopted to obtain higher reflectivity with less sensitivity to injected energy. In order to ensure the amplification effect, length of the SBS cell in Figure 2a,b should be no less than shortest theoretical length L :

$$L = \frac{\tau \cdot c}{2n} \quad (1)$$

where τ is the pump pulse duration at full width at half maximum (FWHM), c is the light speed, n is the refractive index of SBS medium. Figure 2c is the compact single-cell structure involving a concave mirror coated for high reflectivity at pump wavelength that redirects the generated Stokes light through the same cell for amplification. In this structure, the standing-wave field formed by the forward transmission pump light and backward transmission Stokes light can enhance the stability of SBS generation, then improve the stability of the pulse compression; meanwhile, can also effectively compress the cell length [19–21].

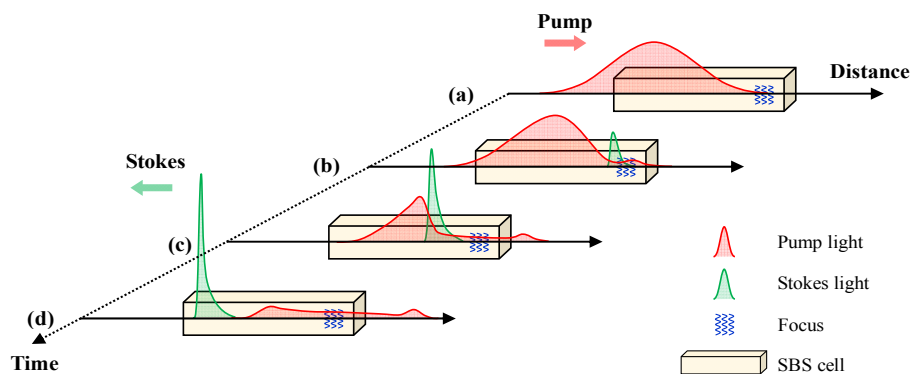


Figure 1. Temporal schematic diagram of simulated Brillouin scattering (SBS) pulse compression process (a) pump light incident to the SBS Cell; (b) backward Stokes light produced near the focus; (c) pump light energy transfer to the leading edge of the Stokes light; (d) compressed Stokes light obtained with a sharp rising edge.

Although many studies on SBS pulse compression technology have been carried out, most people have just paid attention to the pulse compression ratio. Moreover, most of the light sources used in their previous studies are commercial lasers, and there is no combination of the laser amplifier. To the best of our knowledge, little research on the beam quality, stability and applicability of the SBS pulse compression laser has been carried out.

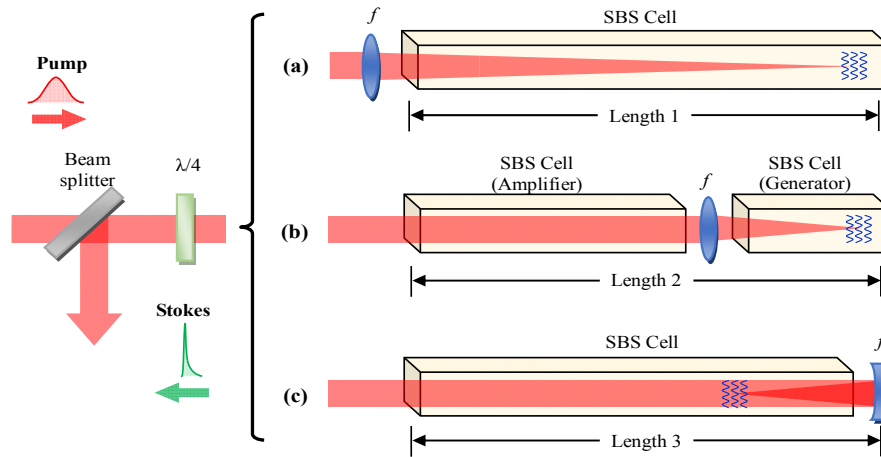


Figure 2. Three kinds of pulse compression device based on SBS technology (a) single-cell structure; (b) two-cell structure; (c) compact single-cell structure. Beam splitter: polarizing plate or polarizing prism; $\lambda/4$: quarter wave plate.

In this paper, we present a compact high beam quality hundred picoseconds laser system based on SBS pulse compression and aberration compensation techniques. Three-plan resonant reflector method is used to generate SLM Q-switched output combined with $\text{Cr}^{4+}:\text{Y}_3\text{Al}_5\text{O}_{12}$ ($\text{Cr}^{4+}:\text{YAG}$) crystal as saturable absorber. Double-pass amplifier is equipped with a compact single-cell SBS pulse compressor in our design. Multi-constituent medium FC-770 is used in the compressor for its high reflectivity and relatively low price. SLM seed pulses of 9 mJ energy with 7.8 ns pulse width are produced from the oscillator. After passing through the SBS pulse compressor, 7.8 ns pulses are then compressed to less than 500 ps by the SBS pulse compressor. The output energy and compressed pulse width as a function of operating voltages are given. Maximum energy 200 mJ is obtained with beam quality factor M^2 less than 1.8 and energy fluctuation measured less than 3%.

2. Experimental Section

The experimental setup of the hundred picoseconds laser system based on SBS pulse compression is shown in Figure 3. The laser system is composed of a SLM oscillator, an optical isolator, a beam expander and a SBS pulse compressor.

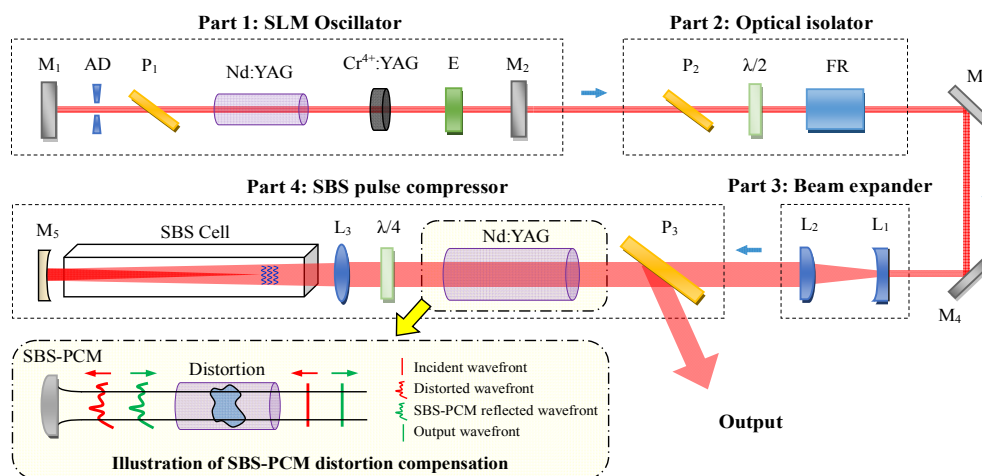


Figure 3. Schematic layout of the hundred picoseconds laser system. SLM: single longitudinal mode; SBS-PCM: Stimulated Brillouin scattering phase conjugation mirror; FR: Faraday rotator; YAG: $\text{Y}_3\text{Al}_5\text{O}_{12}$.

Part 1 is the flash-lamp-pumped SLM oscillator based on three-plan resonant reflector. The $\text{Nd}^{3+}:\text{Y}_3\text{Al}_5\text{O}_{12}$ (Nd:YAG) rod has a length of 120 mm and a diameter of 3 mm with a 1.0% Nd^{3+} concentration. The oscillator is passively Q-switched by a $\text{Cr}^{4+}:\text{YAG}$ crystal with initial transmittance 7.5%. Lower transmittance of the saturable absorber can guarantee the Q-switched output with narrower linewidth and pulse width. The laser cavity is a compact plane-plane configuration with cavity length of 480 mm. M_1 is a 0° concave high reflectivity (HR) mirror at 1064 nm. M_2 is a flat mirror with reflectivity of 50% at 1064 nm as an output coupler (OC). A Fabry–Perot (F-P) etalon E with the thickness of 2 mm is inserted into the cavity to restrict the SLM output through the interaction with the output mirror M_2 , which is equivalent to a composite etalon. P_1 is a Brewster angle polarizer. An aperture diaphragm (AD) is used to filter high-order mode.

Part 2 is the optical isolator, consisting a polarizer P_2 , a $1/2$ wave-plate and a Faraday rotator (FR), used to guarantee the stability of the system by preventing backward Stokes returning to the oscillator.

Part 3 is the beam expander system with a factor of 2 expands the diameter of the laser beam from oscillator.

Part 4 is the SBS pulse compressor consists of a flash-lamp-pumped Nd:YAG amplifier and a SBS cell. 1.0% doped Nd:YAG crystal with a diameter of 7 mm and a length of 140 mm is used as gain medium. FC-770 is chosen as the SBS medium in the SBS cell, which is a multi-constituent perfluorinated compound with molecular formula of $\text{C}_7\text{F}_{15}\text{NO}$. FC-770 has the characteristics of low phonon lifetime (0.57 ns), small Brillouin frequency shift (1081 MHz) and moderate gain coefficient (3.5 cm/GW), which is a suitable medium for SBS pulse compression [22,23]. To reduce the optical breakdown caused by impurities, we filter the FC-770 medium in a vacuum using two layers Millipore filter with pore size 0.05 μm . Stimulated Brillouin scattering phase conjugation mirror (SBS-PCM) and pulse compressor are two primary functions of the SBS cell in our experiment. As a PCM, it can compensate the phase distortion caused by thermal effect and inhomogeneity of the gain crystal [24]. As the illustration of SBS-PCM distortion compensation shows, optical distortion occurred when the seed light (red line) first passes through the laser medium. Due to phase reversal property of the SBS-PCM, after double passing through the optical component, distorted light can be recovered to diffraction-limited (green line) as the original. Meanwhile, the reflected light path from SBS-PCM is strictly same as the incident path, no matter what angle of the SBS cell placed or changed. These remarkable characteristic is helpful for us to realize high beam quality amplified output with high stability. As a pulse compressor, the SBS cell can realize the high efficiency pulse compression of the high energy pulses. The adopted structure of the SBS compressor in our design is a compact single-cell. The length of the SBS cell is 600 mm. To obtain higher reflectance, high compression ratio and sufficient acting length, we insert a convex lens L_3 with focal length 1000 mm in front of the SBS cell. M_5 is a concave total reflection mirror at 1064 nm with focal length 500 mm. After passing through M_5 , pump light is focused on the position close to the near incident end of the cell, producing the backward scattering Stokes light. Based on calculation, the beam size at the focus is about 1.6 mm. Through a $1/4$ wave-plate, backward Stokes light is reflected from the polarizer P_3 with polarization angle rotated from p - to s -polarized.

3. Results and Discussion

The SLM oscillator provides 7.8 ns laser pulses with single pulse energy of 9 mJ at 1064 nm wavelength. The repetition rate of the oscillator is adjustable from 1 to 10 Hz. Figure 4 shows the SLM seed pulse and compressed Stokes pulse we obtained in our experiment, respectively. The waveform of the oscillator output was given in Figure 4a showing a rather smooth shape. The diameters of the oscillator output is about 2.3 mm with angle of divergence less than 0.5 mrad. The temporal profile of the output was detected by a photodetector (UPD-40-UVIR-P; ALPHALAS GmbH, Gottingen, Germany) with rising time less than 40 ps, and recorded by an oscilloscope (806Zi-A; Teledyne LeCory Inc., New York, NY, USA) at a bandwidth of 6 GHz. The compressed pulse profile with steep rising edge and pulse width around 450 ps is shown in Figure 4b.

Figure 5 represents the experimental curve of output energy and compressed pulse width with the change of amplifier voltage, as well as the energy and pulse width stability (error bar). From the curve, we can see that the output energy is near linear growth from 650 to 850 V. One major reason is that with the increase of the injected energy, the SBS reflectivity is obviously improved. The reflectivity we obtained is higher than 75% when the voltage exceeds 650 V. Correspondingly, the output pulse width narrows down rapidly while improving the amplifier voltage from 350 to 650 V. This is because that, at this stage, the leading edge of the Stokes pulse is amplified greatly due to the fast growing gain of the compressor. However, from 700 V to higher voltage, no obvious pulse width compression or changes were observed. The main reason for the increasing energy contributes little to the compression process is that the Stokes pulse width is close to the FC-770 medium phonon lifetime. The measured root mean square error (RMSE) of output energy at 850 V is less than 3%.

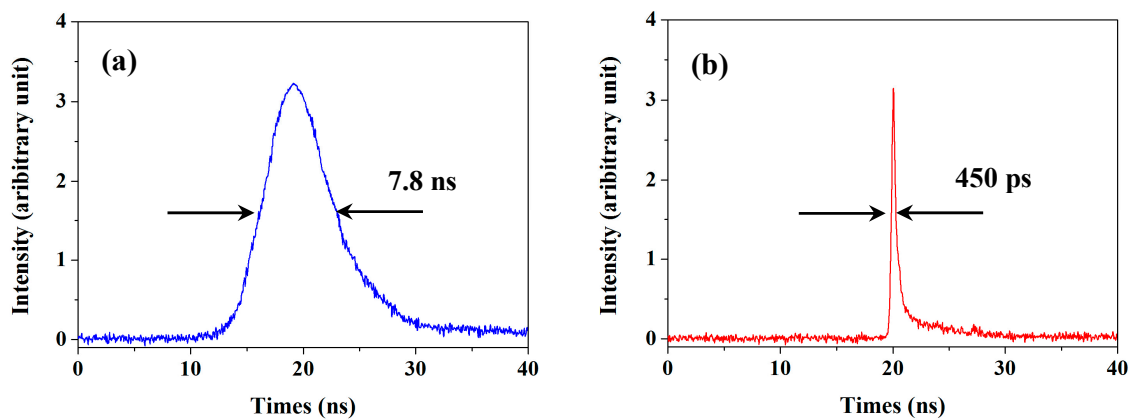


Figure 4. Temporal pulse profiles of the (a) SLM oscillator seed output; (b) SBS pulse width compressed output.

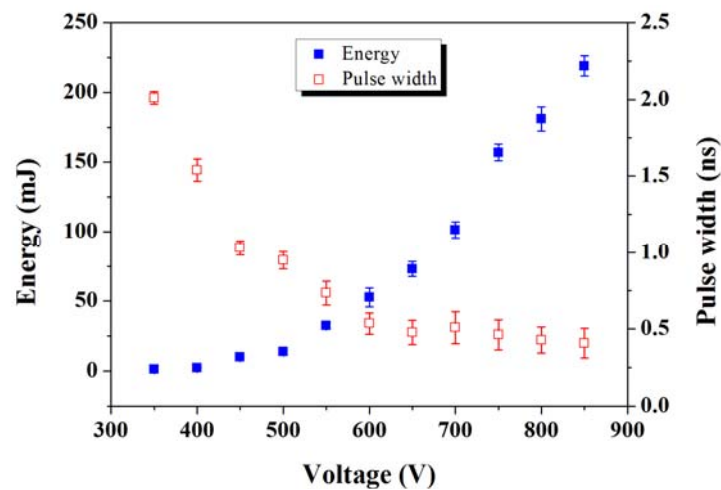


Figure 5. The output energy and pulse width as a function of amplifier voltage.

Figure 6 represents the spatial beam characteristics of the output from polarizer P₃ in both near-field and far-field, which were measured by a Charge Coupled Device (CCD) (Camyu Co. Ltd., Chongqing, China). As shown in Figure 6a,b, the measured beam diameter of near-field is about 6.1 mm in *x*-direction and 5.9 mm in *y*-direction. The near-field beam divergence angle is less than 0.9 mrad. The 2D and 3D far-field laser intensity distribution profiles are given in Figure 6c,d, which obtained by a long focal length lens. Both the near-field and far-field show good beam quality.

Figure 7 shows the measured beam radius under output energy of 200 mJ and pulse width around 450 ps at various distances from the lens with $f = 150$ mm. The transverse output beam profile was measured by using a 90/10 knife-edge technique. The result indicates a beam quality of $M_x^2 = 1.80$, $M_y^2 = 1.75$ in both directions perpendicular to the axis of propagation.

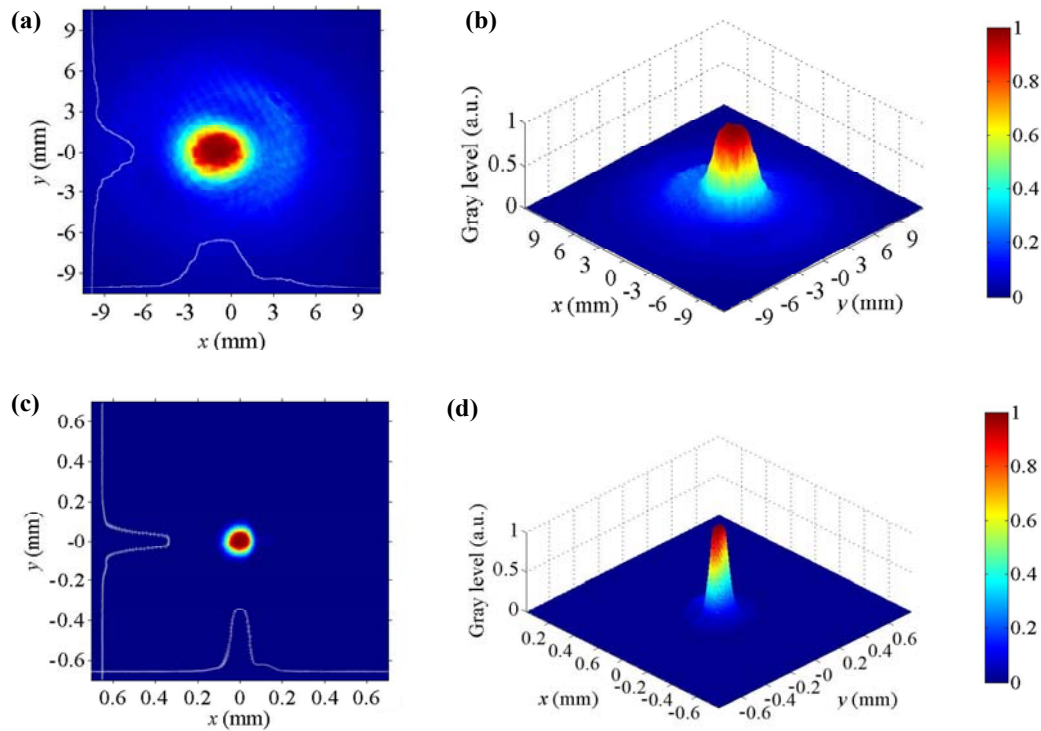


Figure 6. Intensity distribution of SBS pulse width compressed output (a) 2D distribution of near-field; (b) 3D distribution of near-field; (c) 2D distribution of far-field; (d) 3D distribution of far-field.

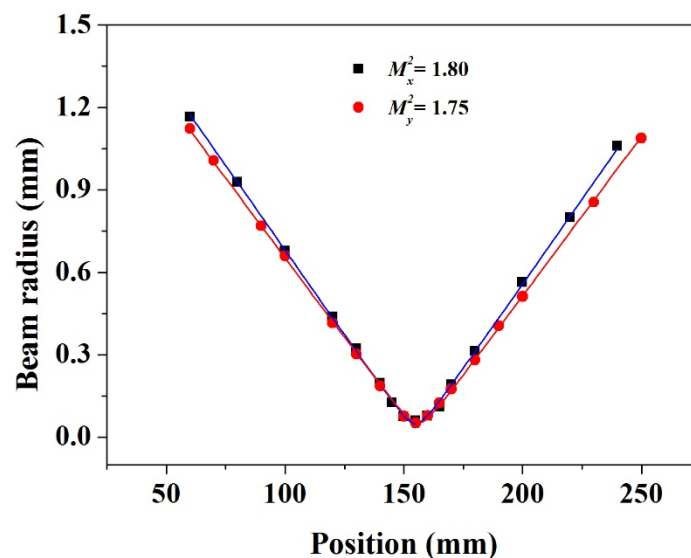


Figure 7. Measured beam characteristics of M^2 with $M_x^2 = 1.80$ and $M_y^2 = 1.75$.

4. Conclusions

In summary, we developed a high beam quality and high compact hundred picoseconds SLM laser system based on SBS phase conjugate compensation and pulse compression technologies.

Compact single-cell structure is adopted in our experiment. By building a standing-wave field with the forward transmission pump light and backward transmission Stokes light, high stability pulse compression is obtained. Owing to the excellent properties of FC-770, these pulses were delivered with a near-diffraction limited spatial intensity profile. Also, different output energy and compressed pulse width were compared experimentally. In the operation of the whole system, maximum energy 220 mJ and compressed pulse around 400 ps was achieved with no breakdown of any optical device or media. The overall energy jitter of the system is less than 3%. The excellent energy, stability and transverse beam profile performances make this system a promising candidate for scientific and industrial applications.

Acknowledgments: This work is supported by the National Natural Science Foundation of China (grant Nos. 61378007, 61138005 and 61378016).

Author Contributions: All the authors have made significant contributions to this study and have approved this submission. Zhenxu Bai built the whole system and drafted the main manuscript; Yulei Wang and Zhiwei Lu supervised the research and provided the experimental platform; Hang Yuan and Zhenxing Zheng designed the pulse compressor; Sensen Li, Yi Chen and Zhaohong Liu contributed to the data analysis and results discussion; Can Cui revised the article and responded the reviewer's comment; Hongli Wang and Rui Liu recorded the experimental data.

Conflicts of Interest: The authors declare no conflict of interest.

References

1. Stuart, B.C.; Feit, M.D.; Herman, S.; Rubenchik, A.M.; Shore, B.W.; Perry, M.D. Nanosecond-to-femtosecond laser-induced breakdown in dielectrics. *Phys. Rev. B* **1996**, *53*, 1749–1761. [[CrossRef](#)]
2. Chichkov, B.N.; Momma, C.; Nolte, S.; Alvensleben, F.; Tünnermann, A. Femtosecond, picosecond and nanosecond laser ablation of solids. *Appl. Phys. A* **1996**, *63*, 109–115. [[CrossRef](#)]
3. Yang, F.M.; Chen, W.Z.; Zhang, Z.P.; Chen, J.P.; Hu, J.F.; Li, X.; Prochazka, I.; Hamal, K. Satellite laser ranging experiment with sub-centimeter single-shot ranging precision at Shanghai Observatory. *Sci. China Ser.* **2003**, *46*, 84–88. [[CrossRef](#)]
4. Amarchinta, H.K.; Grandhi, R.V.; Clauer, A.H.; Langer, K.; Stargel, D.S. Simulation of residual stress induced by a laser peening process through inverse optimization of material models. *J. Mater. Process. Technol.* **2010**, *210*, 1997–2006. [[CrossRef](#)]
5. Li, S.S.; Wang, Y.L.; Lu, Z.W.; Ding, L.; Du, P.Y.; Chen, Y.; Zheng, Z.X.; Ba, D.X.; Dong, Y.K.; Yuan, H.; *et al.* High-quality near-field beam achieved in a high-power laser based on SLM adaptive beam-shaping system. *Opt. Express* **2015**, *23*, 681–689. [[CrossRef](#)]
6. Keller, U.; Weingarten, K.J.; Kartner, F.X.; Kopf, D.; Braun, B.; Jung, I.D.; Fluck, R.; Honninger, C.; Matuschek, N.; der Au, J.A. Semiconductor saturable absorber mirrors (SESAM's) for femtosecond to nanosecond pulse generation in solid-state lasers. *IEEE J. Sel. Top. Quant.* **1996**, *2*, 435–453. [[CrossRef](#)]
7. McDonagh, L.; Wallenstein, R.; Nebel, A. 111 W, 110 MHz repetition-rate, passively mode-locked TEM₀₀ Nd:YVO₄ master oscillator power amplifier pumped at 888 nm. *Opt. Lett.* **2007**, *32*, 1259–1261. [[CrossRef](#)]
8. Zhu, J.F.; Gao, Z.Y.; Tian, W.L.; Wang, J.L.; Wang, Z.H.; Wei, Z.Y.; Zheng, L.H.; Su, L.B.; Xu, J. Kerr-lens mode-locked femtosecond Yb:GdYSiO₅ laser directly pumped by a laser diode. *Appl. Sci.* **2015**, *5*, 817–824. [[CrossRef](#)]
9. Siebold, M.; Hornung, M.; Hein, J.; Paunescu, G.; Sauerbrey, R.; Bergmann, T.; Hollemann, G. A high-average-power diode-pumped Nd:YVO₄ regenerative laser amplifier for picosecond-pulses. *Appl. Phys. B* **2004**, *78*, 287–290.
10. Metzger, T.; Schwarz, A.; Teisset, C.Y.; Sutter, D.; Killi, A.; Kienberger, R.; Krausz, F. High-repetition-rate picosecond pump laser based on a Yb:YAG disk amplifier for optical parametric amplification. *Opt. Lett.* **2009**, *34*, 2123–2125. [[CrossRef](#)]
11. Wegner, U.; Meier, J.; Lederer, M.J. Compact picosecond mode-locked and cavity-dumped Nd:YVO₄ laser. *Opt. Express* **2009**, *17*, 23098–23103. [[CrossRef](#)]
12. Bai, Z.A.; Fan, Z.W.; Bai, Z.X.; Lian, F.Q.; Kang, Z.J.; Lin, W.R. Optical fiber pumped high repetition rate and high power Nd:YVO₄ picosecond regenerative amplifier. *Appl. Sci.* **2015**, *5*, 359–366. [[CrossRef](#)]

13. Omatsu, T.; Kong, H.J.; Park, S.; Cha, S.; Yoshida, H.; Tsubakimoto, K.; Fujita, H.; Miyanaga, N.; Nakatsuka, M.; Wang, Y. The current trends in SBS and phase conjugation. *Laser Prat. Beams* **2012**, *30*, 117–174. [[CrossRef](#)]
14. Damzen, M.J.; Hutchinson, M.H.R. High-efficiency laser-pulse compression by stimulated Brillouin scattering. *Opt. Lett.* **1983**, *8*, 313–315. [[CrossRef](#)]
15. Xu, X.Z.; Feng, C.Y.; Diels, J.C. Optimizing sub-ns pulse compression for high energy application. *Opt. Express* **2014**, *22*, 13904–13915. [[CrossRef](#)]
16. Yoshida, H.; Hatae, T.; Fujita, H.; Nakatsuka, M.; Kitamura, S. A high-energy 160-ps pulse generation by stimulated Brillouin scattering from heavy fluorocarbon liquid at 1064 nm wavelength. *Opt. Express* **2009**, *17*, 13654–13662. [[CrossRef](#)]
17. Dane, C.B.; Neuman, W.A.; Hackel, L.A. High-energy SBS pulse compression. *IEEE J. Quantum Elect.* **1994**, *30*, 1907–1915. [[CrossRef](#)]
18. Schiemann, S.; Ubachs, W.; Hogervorse, W. Efficient temporal compression of coherent nanosecond pulses in a compact SBS generator-amplifier setup. *IEEE J. Quantum Elect.* **1997**, *33*, 358–366. [[CrossRef](#)]
19. Neshev, D.; Velchev, I.; Majewski, W.A.; Hogervorst, W.; Ubachs, W. SBS pulse compression to 200 ps in a compact single-cell setup. *Appl. Phys. B* **1999**, *68*, 671–675. [[CrossRef](#)]
20. Schiemann, S.; Hogervorst, W.; Ubachs, W. Fourier-transform-limited laser pulses tunable in wavelength and in duration (400–2000 ps). *IEEE J. Quantum Elect.* **1998**, *34*, 407–412. [[CrossRef](#)]
21. Velchev, I.; Ubachs, W. Statistical properties of the Stokes signal in stimulated Brillouin scattering pulse compressors. *Phys. Rev. A* **2005**, *71*, 043810. [[CrossRef](#)]
22. Hasi, W.L.J.; Qiao, Z.; Cheng, S.X.; Wang, X.Y.; Zhong, Z.M.; Zheng, Z.X.; Lin, D.Y.; He, W.M.; Lu, Z.W. Characteristics of SBS hundreds picosecond pulse compression and influence of energy on pulse stability in FC-770. *Opt. Commun.* **2013**, *311*, 375–379. [[CrossRef](#)]
23. Yuan, H.; Lu, Z.W.; Wang, Y.L.; Zheng, Z.X.; Chen, Y. Hundred picoseconds laser pulse amplification based on scalable two-cells Brillouin amplifier. *Laser Prat. Beams* **2014**, *32*, 369–374. [[CrossRef](#)]
24. Brignon, A.; Huignard, J.P. *Phase Conjugate Laser Optics*, 1st ed.; John Wiley, Inc.: Hoboken, NJ, USA, 2004.



© 2016 by the authors; licensee MDPI, Basel, Switzerland. This article is an open access article distributed under the terms and conditions of the Creative Commons by Attribution (CC-BY) license (<http://creativecommons.org/licenses/by/4.0/>).